

**Contract No:**

This document was prepared in conjunction with work accomplished under Contract No. DE-AC09-08SR22470 with the U.S. Department of Energy (DOE) Office of Environmental Management (EM).

**Disclaimer:**

This work was prepared under an agreement with and funded by the U.S. Government. Neither the U. S. Government or its employees, nor any of its contractors, subcontractors or their employees, makes any express or implied:

- 1 ) warranty or assumes any legal liability for the accuracy, completeness, or for the use or results of such use of any information, product, or process disclosed; or
- 2 ) representation that such use or results of such use would not infringe privately owned rights; or
- 3) endorsement or recommendation of any specifically identified commercial product, process, or service.

Any views and opinions of authors expressed in this work do not necessarily state or reflect those of the United States Government, or its contractors, or subcontractors.



# Compression Stress-Relaxation and Oxygen Consumption Behavior of 9975 Shipping Package O-rings

T.-T. Truong

W. L. Daugherty

May 2018

SRNL-STI-2018-00201, Revision 0



## **DISCLAIMER**

This work was prepared under an agreement with and funded by the U.S. Government. Neither the U.S. Government or its employees, nor any of its contractors, subcontractors or their employees, makes any express or implied:

1. warranty or assumes any legal liability for the accuracy, completeness, or for the use or results of such use of any information, product, or process disclosed; or
2. representation that such use or results of such use would not infringe privately owned rights; or
3. endorsement or recommendation of any specifically identified commercial product, process, or service.

Any views and opinions of authors expressed in this work do not necessarily state or reflect those of the United States Government, or its contractors, or subcontractors.

**Printed in the United States of America**

**Prepared for  
U.S. Department of Energy**

**Keywords:** *9975 Shipping Package*  
*O-ring*  
*Oxidation*

**Retention:** *Permanent*

# **Compression Stress-Relaxation and Oxygen Consumption Behavior of 9975 Shipping Package O-rings**

T.-T. Truong  
W. L. Daugherty

May 2018

---

Prepared for the U.S. Department of Energy under  
contract number DE-AC09-08SR22470.



## EXECUTIVE SUMMARY

The 9975 shipping package is used within the DOE complex for shipping special nuclear materials. The shipping packages are currently approved for up to 20 years storage in K-Area Complex (KAC) and work continues to provide technical basis to extend that period. Several techniques have been used at Savannah River National Laboratory to monitor the aging performance of Viton® GLT or GLT-S fluoroelastomer O-rings. These experiments all involve accelerated aging of the O-ring samples at elevated temperatures. This report describes efforts to extend the service life estimate of GLT and GLT-S O-rings used in the 9975 shipping package.

A series of experiments have been ongoing to assess the compression stress-relaxation (CSR) performance of GLT and GLT-S O-rings at elevated temperatures from 175 to 400 °F and the oxygen consumption behavior of GLT-S O-rings at 73 to 250 °F. The CSR and oxygen consumption data were used to develop predictive models for extrapolation of CSR behavior to bounding O-ring temperatures ( $\leq 158$  °F) during storage in the K-Area Complex. Oxygen consumption results at low temperatures, below 175 °F, provided confidence in the extrapolation of O-ring behavior to KAC storage temperatures. The predictive model using time-temperature superposition estimates the service life at 158 °F is 34 years and 570 years for GLT and GLT-S O-rings, respectively.

For samples aged at the same temperature range, 175 to 250 °F, data from oxygen consumption are generally in agreement with results from compression stress-relaxation testing. Additionally, the oxygen consumption measurements are sufficiently sensitive to allow meaningful and timely measurements at lower temperatures, well within the range of KAC service temperatures. These results provide increased confidence in O-ring service life estimates by demonstrating that extrapolations of the mechanical test results to KAC service temperatures are valid. However, uncertainty still exists in extrapolating these elevated temperature results to the KAC service temperatures due to sample variation in testing results and the effect of diffusion-limited oxidation on the samples. Aging and CSR testing will continue for GLT and GLT-S O-ring samples at 175 and 250 °F. Aging and oxygen consumption testing will continue for GLT-S O-ring samples at 73 to 250 °F.

## TABLE OF CONTENTS

LIST OF TABLES .....	vii
LIST OF FIGURES .....	vii
LIST OF ABBREVIATIONS.....	viii
1.0 Introduction.....	1
2.0 Experimental Procedure.....	1
3.0 Results and Discussion .....	4
4.0 Conclusions.....	11
5.0 References.....	12
Appendix A.....	A-1

## LIST OF TABLES

Table 1. Extrapolated lifetimes for GLT and GLT-S O-rings based on the time to reach $0.1F_o$ . ....	8
--	---

## LIST OF FIGURES

Figure 1. Schematic (a) and photograph (b) of the oxygen analyzer system. ....	2
Figure 2. Photograph of the oxygen consumption sample vessel. ....	3
Figure 3. Example of oxygen concentration curves for the sample and reference air flows and the oxygen deficit (shaded area).....	4
Figure 4. Representative normalized CSR values ( $F/F_o$ ) for GLT O-rings aged at different temperatures over time. ....	5
Figure 5. Representative normalized CSR values ( $F/F_o$ ) for GLT-S O-rings aged at different temperatures over time. ....	5
Figure 6. Normalized CSR values ( $F/F_o$ ) for all tested GLT O-rings aged at different temperatures over time (a) and time-temperature superposition of CSR data relative to 175 °F, $a_T=1$ (b).....	6
Figure 7. Normalized CSR values ( $F/F_o$ ) for all tested GLT-S O-rings aged at different temperatures over time (a) and time-temperature superposition of CSR data relative to 175 °F, $a_T=1$ (b). ....	7
Figure 8. The shift factors ( $a_T$ ) for CSR testing of GLT and GLT-S O-ring samples with $a_T= 1$ at 175 °F.7	
Figure 9. The oxygen consumption (a) and time-temperature superposition of oxygen consumption data relative to 175 °F, $a_T=1$ (b) for 0.07 inch thick GLT-S samples.....	8
Figure 10. The shift factors ( $a_T$ ) for oxygen consumption testing of GLT-S samples of various thicknesses with $a_T= 1$ at 175 °F. The dashed lines are projected shift factor values. ....	9
Figure 11. Plot of the shift factors ( $a_T$ ) for CSR and oxygen consumption of GLT-S samples with $a_T= 1$ at 175 °F. The dashed lines are projected shift factor values. ....	10
Figure 12. Plot of the shift factors ( $a_T$ ) for CSR, oxygen consumption (0.13 inch thickness), and leak testing of GLT and GLT-S samples. The dashed lines are projected shift factor values. ....	11

## **LIST OF ABBREVIATIONS**

CSR	Compression stress-relaxation
DLO	Diffusion-limited oxidation
EPDM	Ethylene propylene diene monomer
KAC	K-Area Complex
SRNL	Savannah River National Laboratory
TTS	Time-temperature superposition



## 1.0 Introduction

In the Model 9975 shipping package, used for the transportation of plutonium materials, primary and secondary containment vessels are sealed with dual Viton® GLT or GLT-S fluoroelastomer O-rings. The O-rings are credited for leak-tight containment [1]. The 9975 shipping package is currently approved for a storage period of 20 years in K-Area Complex (KAC) based on thermal and structural calculations [2-5]. This report describes the behavior and degradation trends of O-ring samples conditioned in elevated temperature environments using compression stress-relaxation (CSR) and oxygen consumption testing. The purpose of these experiments is to correlate the performance of O-rings to lifetime predictions of O-ring seals in 9975 shipping packages stored in KAC and assess service life predictions from O-ring leak testing. This is the status report for CSR and oxygen consumption O-ring experiments carried out per Task Technical Plan [6], which is part of the comprehensive 9975 package surveillance program [7].

Compression stress-relaxation tests measure the counterforce exerted by an elastomeric seal over time at a fixed amount of compression. CSR O-ring samples are conditioned at elevated temperatures at Savannah River National Laboratory (SRNL) to accelerate the degradation of the O-rings to observe property changes in a reasonable time-scale. The results of these tests are extrapolated to KAC service temperatures based upon models that assume Arrhenius behavior of O-rings over the temperature regimes (i.e. assume degradation mechanism(s) do not change with temperature). Baseline and long-term testing of CSR behavior through 2015 have been reported previously with estimated service life at 156 °F of 37 and 791 years for GLT and GLT-S O-rings, respectively [8]. Additional data has been collected and the cumulative data set through February 2018 is presented in this report.

The limitation of the Arrhenius method is the possibility that degradation rates observed at elevated temperatures do not extrapolate reliably to lower temperatures due to changes in the degradation mechanisms. Aging samples at lower temperatures could address this limitation but samples might require prohibitively long testing periods to observe degradation or reach a failure point.

Oxygen consumption analysis can measure the oxidation rates of materials at low conditioning temperatures in relatively brief periods of time, as well as at elevated temperatures [9, 10]. Thermo-oxidative processes are the primary degradation mechanisms for many polymers exposed to oxygen-containing environments, and oxidation rates are generally correlated to the rate of degradation of mechanical properties [11]. Oxygen consumption analysis bridges the gap between degradation at service temperatures and elevated temperatures and can corroborate and add confidence to extrapolations of mechanical test results to service conditions.

## 2.0 Experimental Procedure

### *Compression Stress-Relaxation*

CSR behavior is measured per ASTM D6147 using Shawbury-Wallace C11 jigs and a Wallace Mark IV relaxometer. The sealing force is measured periodically as this approach is conducive to longer test periods and realistic aging temperatures. Size 2-213 O-rings were used to fit within the CSR jigs, while matching the thickness of the 9975 O-rings (0.139 inch). To mimic the 9975 O-ring design, the O-rings are tested with a nominal 18% compression imposed during aging. The CSR jigs are aged at 175, 235, 250, 300, 350 °F (both compounds) and 400 °F (GLT-S only). The

only jigs still conditioning as of April 2018 are 175 and 250 °F samples. The CSR jigs are periodically removed from their aging environment to measure the O-ring's counterforce. The CSR results are presented as a force decay ratio ( $F/F_0$ ), with an initial sealing force of  $F_0$ . The values are the average of five sequentially measured counterforce values minus the empty jig break force and normalized to the initial sealing force. The CSR methodology has been previously described in greater detail in reports [8, 12].

### *Oxygen Consumption*

The oxidation rate of materials can be calculated by measuring the oxygen consumption (i.e. uptake of oxygen) by the materials in a closed vessel. The oxygen consumption of O-rings is measured using a differential oxygen analyzer as described in the literature [10]. The oxygen analyzer system consists of a dry air cylinder, two mass flow controllers, multiplexer, fuel cell respirometer, pressure transducer, and vacuum (Figure 1). As it is desirable to maintain a constant

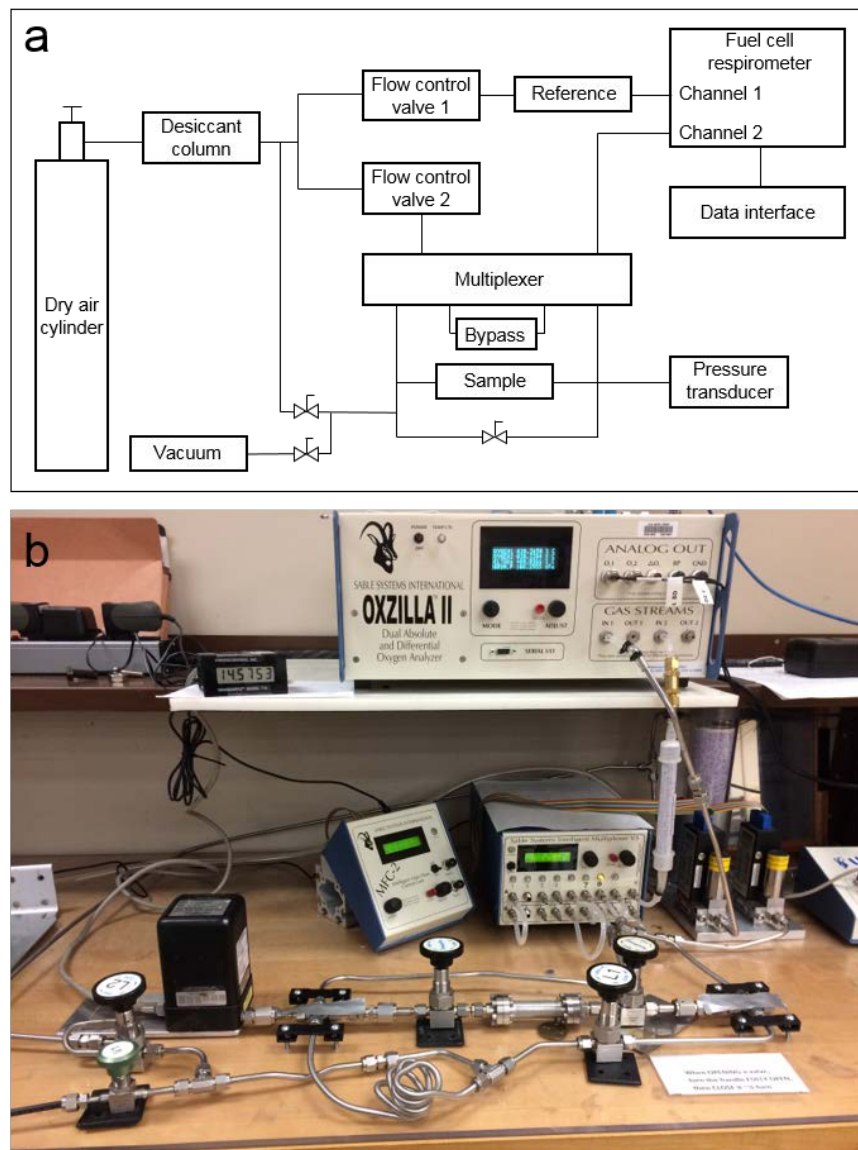


**Figure 1.** Schematic (a) and photograph (b) of the oxygen analyzer system.

rate of oxygen consumption, the sample size, vessel volume, and aging time were selected to minimize the effect of oxygen depletion (i.e. the fraction of oxygen consumed is not significant enough to change the rate of oxidation).

Oxygen consumption samples are typically ~1 x 3/8 inch pieces cut from Viton GLT-S sheets of three different thicknesses of 0.03, 0.07, and 0.13 inches. The pieces were cleaned with alcohol and weighed. The pieces were loaded into mini Conflat flanged vessels sealed with gold-coated copper gaskets and connected to a valve on each end (Figure 2). In addition, an empty vessel was constructed as a control sample, and two vessels contained a piece of ethylene propylene diene monomer (EPDM) for comparison to published data. The vessels were verified to be leak-tight using a helium leak test, and the free volumes were measured by the High Pressure Lab at SRNL.

The sample vessel was connected to a Sable Systems Oxzilla II Dual Absolute and Differential Oxygen Analyzer and flushed with cylinder air at 25 cc/min. The valves of the vessel were closed and the vessel was placed in an oven. After two hours, one of the valves was briefly opened to equilibrate the vessel to atmospheric pressure. This step ensured all samples age at a known pressure of 1 atm and are consistent with the pressure of CSR samples. The vessels are aged at 73, 104, 140, 175, 212, and 250 °F. The information on the sample vessels are listed in Table A-1.

After aging, the sample vessel is connected to the oxygen analyzer system, and the short sections of the system exposed to atmospheric air are evacuated and refilled with cylinder air. After the oxygen concentration in the bypass loop is stabilized, both outputs of the respirometer are set to 20.95% oxygen. Then, air flow is switched from the bypass loop to the sample chamber by the multiplexer and the oxygen concentrations in the reference and sample air flows are measured by the fuel cell respirometer. The oxygen consumed in the sample chamber due to uptake by the polymer is determined by calculating the difference between the two air flow curves (Figure 3). The experiment is continued until the concentration in the air flows match and there are two steady baselines as the cylinder air fully displaced the air in the sample vessel. The empty vessel is evaluated prior to and at the end of testing to verify the oxygen analyzer system is functioning correctly.

The oxygen deficit of the sample vessel (units of scc) is calculated by multiplying the gas flow rate by the integral of the oxygen concentration versus flow time (i.e. shaded area in Figure 3) and

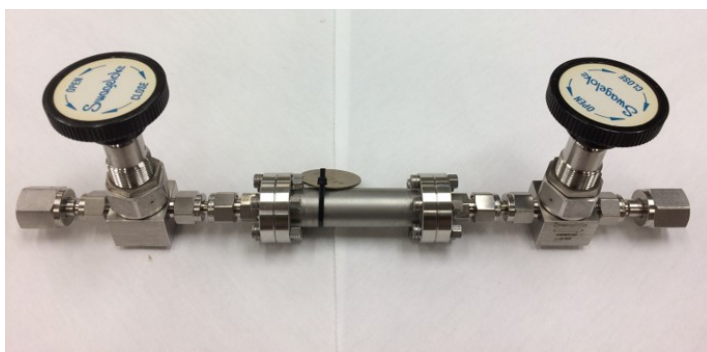


**Figure 2.** Photograph of the oxygen consumption sample vessel.

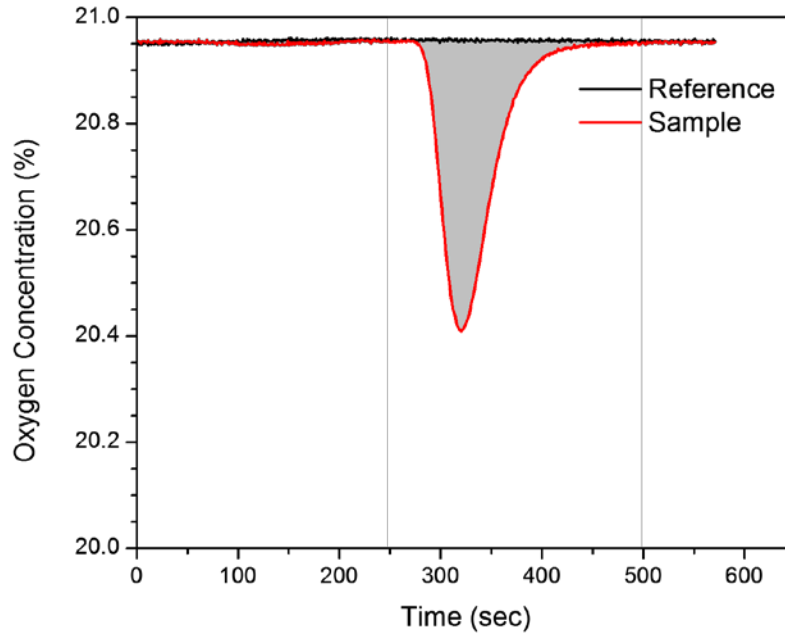


**Figure 3.** Example of oxygen concentration curves for the sample and reference air flows and the oxygen deficit (shaded area).

dividing by 100%. The oxidation rate (units of mole  $O_2$ /g/s) is obtained by converting the volume of oxygen to moles of oxygen and dividing by the sample weight and aging time.

### 3.0 Results and Discussion

The CSR results are presented as a force decay ratio ( $F/F_0$ ), with an initial sealing force of  $F_0$ . Representative CSR values for GLT and GLT-S O-rings conditioned at different temperatures for up to 10 years are shown in Figure 4 and Figure 5, respectively. For both O-ring materials, the force decay ratio decreases more rapidly at higher aging temperatures. The overall trend indicates a quicker decay of the GLT than the GLT-S O-rings at a given temperature, consistent with the previous report [8].

The entire CSR data for GLT and GLT-S O-rings are plotted in Figure 6a and Figure 7a, respectively. The data are used to develop predictive models for extrapolation of CSR behavior to relevant service temperatures (e.g. O-ring temperature of 158 °F [2]) using time-temperature superposition (TTS). For TTS, the time scale for each sample is multiplied by a shift factor,  $a_T$ , until the data superimpose with each other. The reference temperature for the O-ring samples is 175 °F with  $a_T=1$ , and the shift factors are listed in Table A-2. The TTS curves for GLT and GLT-S O-rings are shown in Figure 6b and Figure 7b, respectively. The curves show reasonable agreement in overall curve shape for each O-ring type. The shift factors are plotted as a function of reciprocal temperature in Figure 8 for both O-ring materials. Figure 6 and Figure 7 show sample variation, including differences in curve shape, at a given aging temperature and that is reflected in the vertical spread of shift factors in Figure 8. However, a linear correlation exists for both GLT and GLT-S O-rings which is indicative of Arrhenius behavior as described by the equation,

$$\text{rate constant} = Ae^{\frac{-E_a}{RT}}$$

where A is the Arrhenius constant,  $E_a$  is the activation energy, R is the ideal gas constant, and T is

the absolute temperature. Activation energy is calculated by multiplying the ideal gas constant by the slope of the linear correlation in Figure 8. The calculated activation energies are 58 kJ/mol and 83 kJ/mol for GLT and GLT-S, respectively. The calculated activation energies can be used to

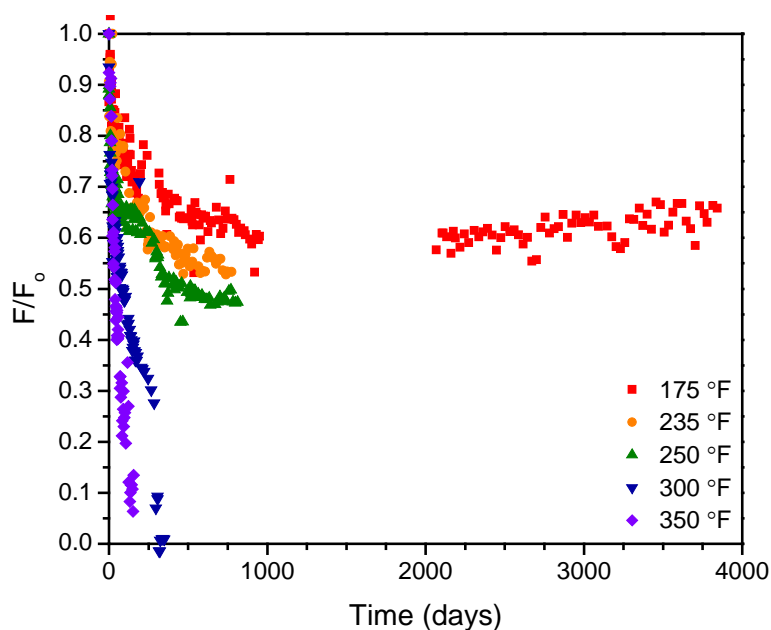


**Figure 4.** Representative normalized CSR values ( $F/F_0$ ) for GLT O-rings aged at different temperatures over time.

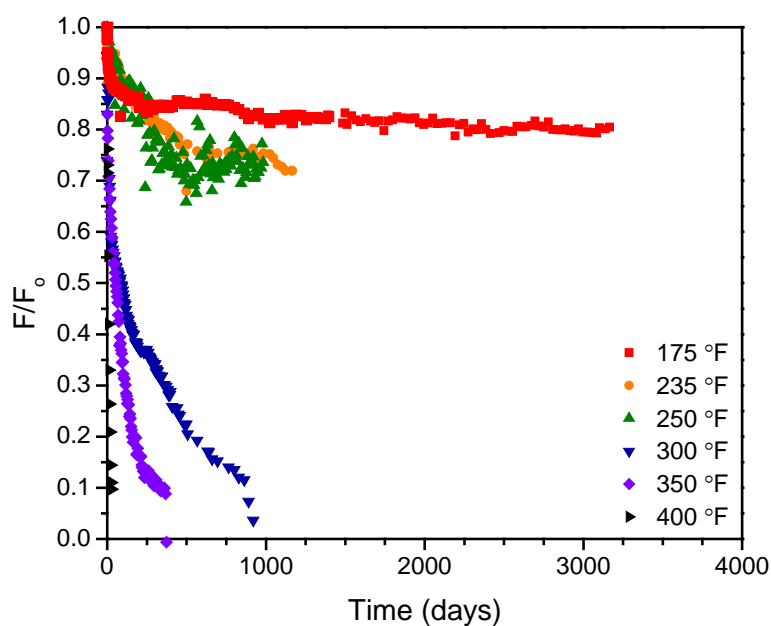


**Figure 5.** Representative normalized CSR values ( $F/F_0$ ) for GLT-S O-rings aged at different temperatures over time.

compare the temperature dependence of degradation for O-ring materials. The CSR data demonstrate GLT O-rings degrade faster at a given temperature than GLT-S O-rings.

The mechanical lifetime of a seal is generally estimated as  $F/F_0 = 0.1$  or 90% loss of counterforce [9, 13]. With the TTS model and calculated activation energy, the time to reach a CSR ratio of  $F/F_0=0.1$  can be extrapolated for any temperature of interest, provided the degradation mechanisms remain constant over the temperature range. At 300 °F, the time required to reach a decay ratio of 0.1 for GLT is approximately 280 days. Using the ratio of shift factors at 300 °F and 158 °F from Figure 8 (25 and 0.56), the extrapolation predicts that it will take 34 years for GLT O-rings aged at 158 °F to reach  $0.1F_0$ . The same process can be applied to various temperatures for GLT and GLT-S O-rings. The extrapolated time to reach  $0.1F_0$  for GLT and GLT-S O-rings are summarized in Table 1. Since this extrapolation is based only on CSR data, it does not include degradation mechanisms or reactions that are not present under the existing testing parameters, such as surface modifications, microcracking, stretching or other effects that could lead to an O-ring leak. In addition, there are differences in curve shape for CSR data (Figure 6-7) which raises questions as to whether there are consistent degradation mechanisms over the temperature range and how reliable the data can be extrapolated. This uncertainty stresses the need to examine oxygen consumption data, which include results for samples aged near KAC service temperatures, to add confidence in the extrapolation.

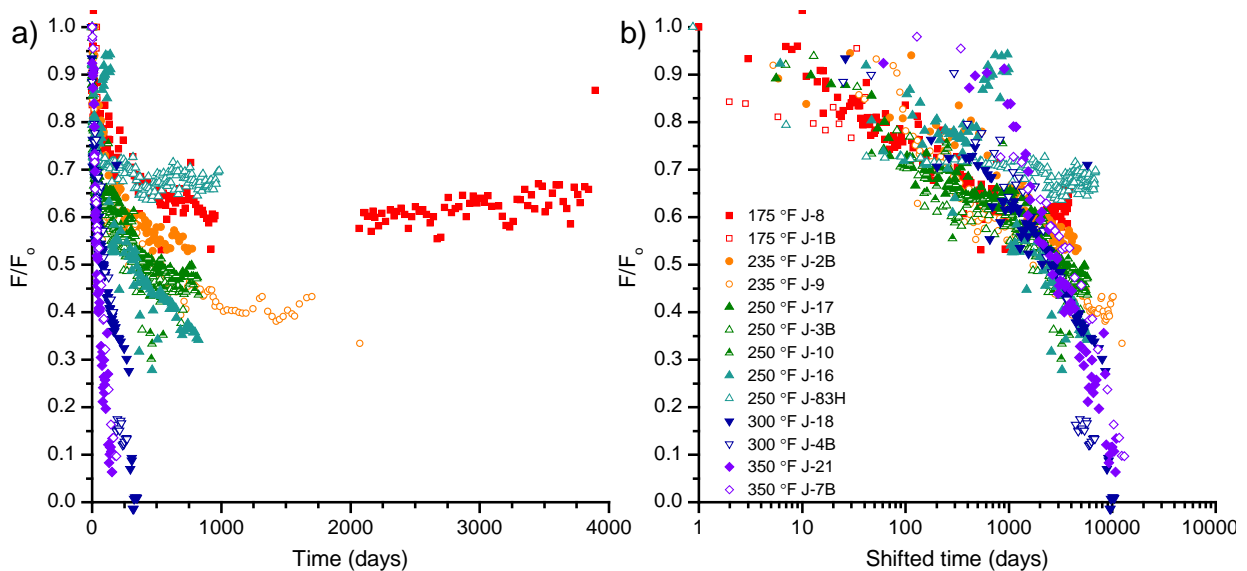


**Figure 6.** Normalized CSR values ( $F/F_0$ ) for all tested GLT O-rings aged at different temperatures over time (a) and time-temperature superposition of CSR data relative to 175 °F,  $a_T=1$  (b).

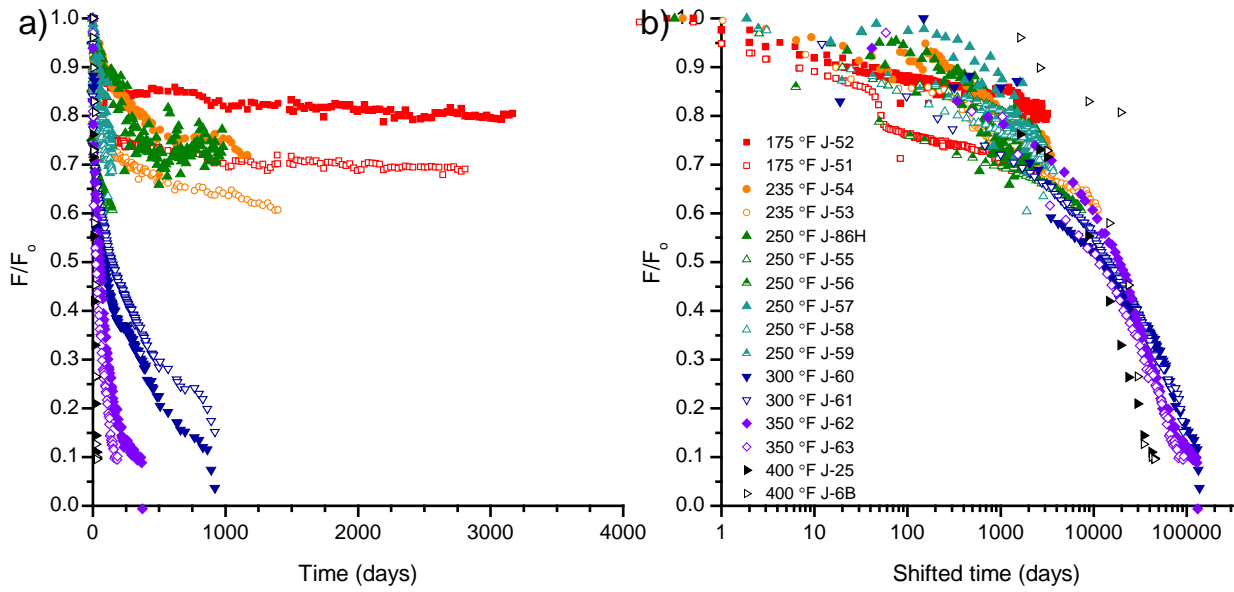


**Figure 7.** Normalized CSR values ( $F/F_0$ ) for all tested GLT-S O-rings aged at different temperatures over time (a) and time-temperature superposition of CSR data relative to 175 °F,  $a_T=1$  (b).

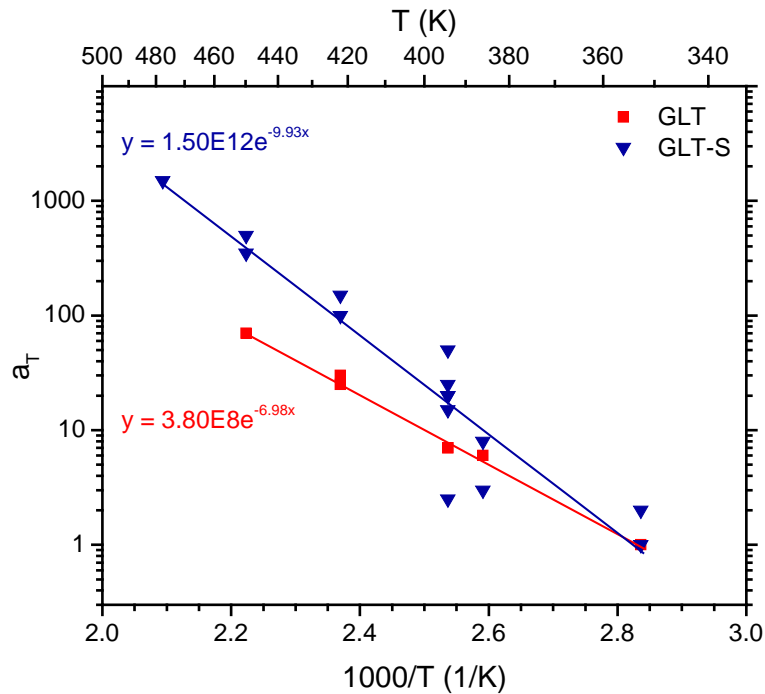


**Figure 8.** The shift factors ( $a_T$ ) for CSR testing of GLT and GLT-S O-ring samples with  $a_T= 1$  at 175 °F.



**Table 1.** Lifetimes and extrapolated lifetimes for GLT and GLT-S O-rings to reach 0.1F<sub>o</sub>.

Temperature (°F)	GLT O-rings		GLT-S O-rings	
	Time to 0.1F <sub>o</sub> (days)	Time to 0.1F <sub>o</sub> (years)	Time to 0.1F <sub>o</sub> (days)	Time to 0.1F <sub>o</sub> (years)
300 °F <sup>a</sup>	280	1	1,270	3
250 °F <sup>b</sup>	900	2	6,670	18
235 °F <sup>b</sup>	1320	4	11,480	31
175 °F <sup>b</sup>	7,290	20	130,770	358
158 °F <sup>c</sup>	12,570	34	283,880	778
150 °F <sup>c</sup>	16,420	45	415,000	1,137
125 °F <sup>c</sup>	39,630	109	1,453,720	3,983
100 °F <sup>c</sup>	103,490	284	5,695,680	15,605

<sup>a</sup> Samples reached 0.1F<sub>o</sub>.

<sup>b</sup> Data extrapolated to 0.1F<sub>o</sub>.

<sup>c</sup> No CSR data at this temperature, extrapolation based upon predictive model

Oxygen consumption analysis is another method to evaluate and model the degradation of O-rings. Polymer samples are enclosed in a vessel filled with air and allowed to oxidize at different temperatures. After the aging period, the oxygen depletion (i.e. amount of oxygen consumed by the sample) is measured by the oxygen analyzer system. Oxygen consumption values for 0.07 inch thick GLT-S O-rings conditioned at different temperatures are shown in Figure 9a. The slopes of the oxygen consumption data for samples aged from 73 to 250 °F are similar and indicate that time-temperature superposition is possible. Note that the time scales are reasonable (under 2 months) for most of the aging temperatures, except for the room temperature samples. Also, the oxygen consumption rates at each aging temperature are relatively constant as shown in Figure A-1

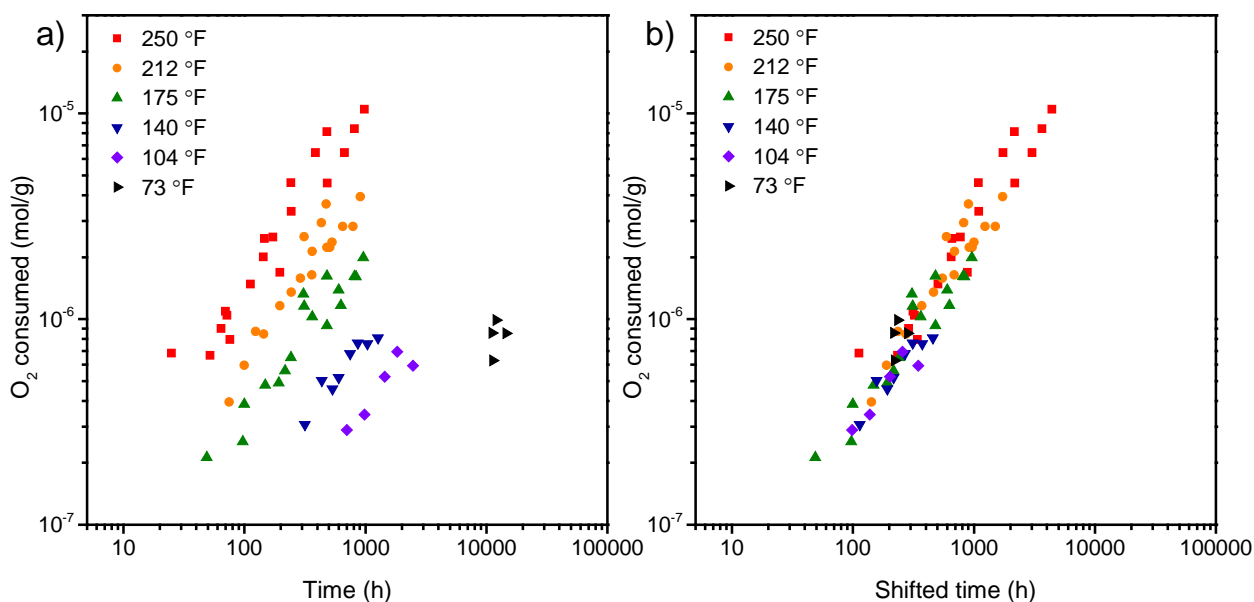


**Figure 9.** The oxygen consumption (a) and time-temperature superposition of oxygen consumption data relative to 175 °F,  $a_T=1$  (b) for 0.07 inch thick GLT-S samples.



which indicate the degradation mechanism did not change with aging time. The time-temperature superposition plot is shown in Figure 9b. The data points superimpose reasonably well. The oxygen consumption and time-temperature superposition plots for 0.03 and 0.13 inch thick GLT-S O-rings are shown in Figure A-2 and Figure A-4, respectively. The shift factors for all oxygen consumption samples are listed in Table A-2.

The TTS curves for 0.03, 0.07, and 0.13 inch thick GLT-S O-rings are shown in Figure 10. The shift factors for samples aged at room temperature are not shown due to small sample size. The TTS slopes get steeper as the sample thickness increases which corresponds to different activation energies. The calculated activation energies are 33, 44, and 55 kJ/mol for 0.03, 0.07, and 0.13 inch thick GLT-S O-rings, respectively. The different activation energies are due to diffusion-limited oxidation (DLO) effect where the material consumes oxygen faster than it can be replaced by diffusion from the surrounding atmosphere. This leads to equilibrium oxidation at the surface and diminished oxidation away from the surface. The oxygen consumption results are biased to indicate oxidation occurred less in samples affected by DLO (i.e. thicker samples), and estimate higher activation energies and predict longer service lifetimes. The impact of diffusion-limited oxidation is clearly shown in Figure 10 and thinner samples can be used to reduce DLO effects. However, it should be noted that O-rings in CSR, leak testing, and 9975 package have limited free surface area exposed to oxygen atmosphere due to contact with vessels and might be better represented by the thicker samples that show greater DLO effects.

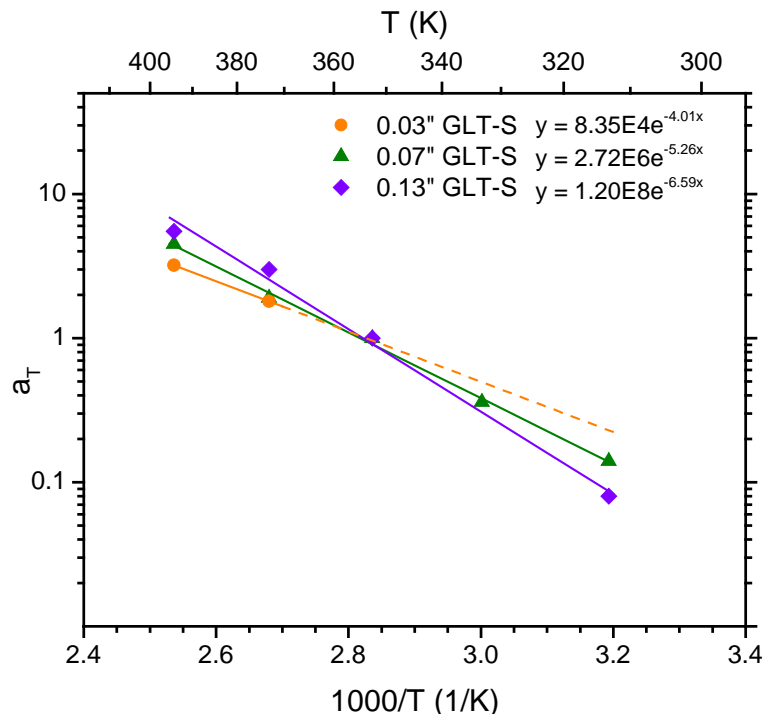


**Figure 10.** The shift factors ( $a_T$ ) for oxygen consumption testing of GLT-S samples of various thicknesses with  $a_T = 1$  at 175 °F. The dashed lines are projected shift factor values.

The time-temperature superposition plot for CSR and oxygen consumption of GLT-S O-ring samples is shown in Figure 11. The shift factors for oxygen consumption of GLT-S O-rings are within the sample variation range for CSR results. The thickest GLT-S oxygen consumption sample (0.13 inch) is closest in agreement with CSR shift factors. CSR O-ring samples are originally 0.14 inch thick but are compressed and in contact with metal jigs during aging. This aging condition limits the exposure to oxygen, better mimicking the conditions in the 9975 containment vessel seal design. Figure 11 indicates the CSR results could be strongly impacted by DLO effects as the O-rings are thicker than oxygen consumption samples and the experimental set up reduces oxygen availability to the compressed O-rings. Since the oxygen consumption data deviate from the extrapolated CSR data at temperatures below 175 °F, there may be a change in degradation mechanisms and activation energy at this lower temperature range. One might explore this by using the oxygen consumption shift factors to extrapolate CSR data to make predictions at KAC service temperatures ( $a_T = 0.54$  at 158 °F). In this case, the extrapolation predicts that it will take 586 years for GLT-S O-rings aged at 158 °F to reach 0.1F<sub>o</sub>. This is slightly less than the prediction of 778 years based upon only CSR data.

Leak testing of O-ring fixtures has been ongoing for 11 years at SRNL. Leak test data have been used to estimate the O-rings should maintain a leak-tight seal for up to 77 years aging at 200 °F and have a greater service life at KAC storage temperatures [14]. Oxygen consumption shift factors at service temperatures can be used to compare extrapolations of CSR and leak testing results. The shift factors for CSR, oxygen consumption, and leak testing of GLT and GLT-S O-ring samples are shown in Figure 12. The shift factors for leak testing were calculated based on the time to failure results [14]. The time to failure for O-ring fixtures were normalized to the time to failure

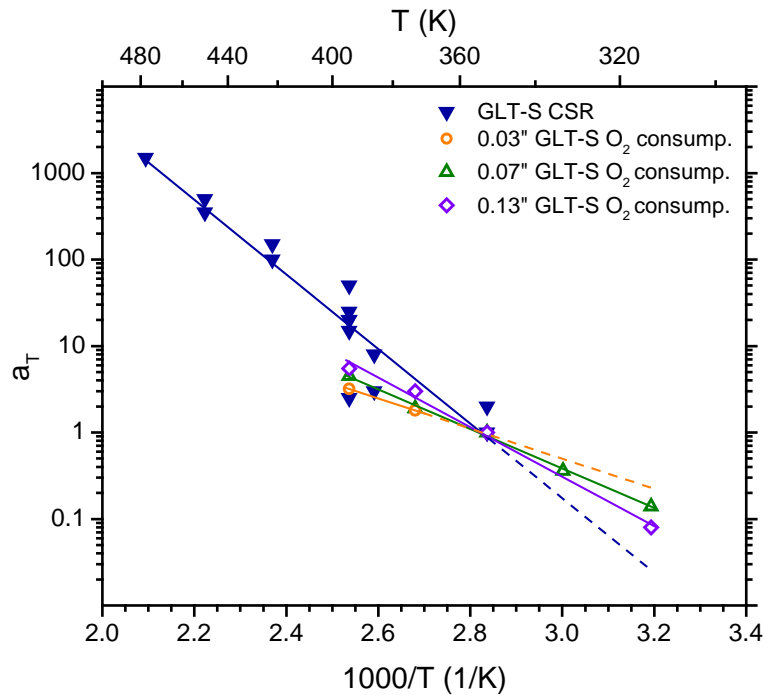


**Figure 11.** Plot of the shift factors ( $a_T$ ) for CSR and oxygen consumption of GLT-S samples with  $a_T = 1$  at 175 °F. The dashed lines are projected shift factor values.

of fixtures aged at 300 °F, and then shifted by a conversion factor to obtain shift factors relative to  $a_T = 1$  at 175 °F as shown in Table A-3.

The dashed red line in Figure 12 is the projection based upon the lowest time to failure for both GLT and GLT-S O-ring leak testing results. The projection estimates O-rings aging at 158 °F might maintain a leak-tight seal for up to 570 years. This corresponds well with the prediction of 586 years using both CSR and oxygen consumption TTS results. The oxygen consumption shift factors correlate well with the CSR extrapolation for GLT O-ring samples, and bound the shift factors from CSR extrapolation of GLT-S O-ring samples. If the assumption is made that GLT and GLT-S O-rings have similar oxygen consumption behavior, then oxygen consumption results support the CSR service life estimation of 34 years at 158 °F for GLT O-rings. Additional oxygen consumption tests with GLT O-rings can verify the validity of the assumption and improve the service life prediction.

Two vessels with EPDM samples have also been examined to verify the testing and analysis matched literature results. The oxygen consumption and time-temperature superposition of EPDM samples are shown in Figure A-6. The shift factors and calculated activation energy of 75 kJ/mol for oxygen consumption data of EPDM matched reasonably well with those reported in the literature (Figure A-8) [15].

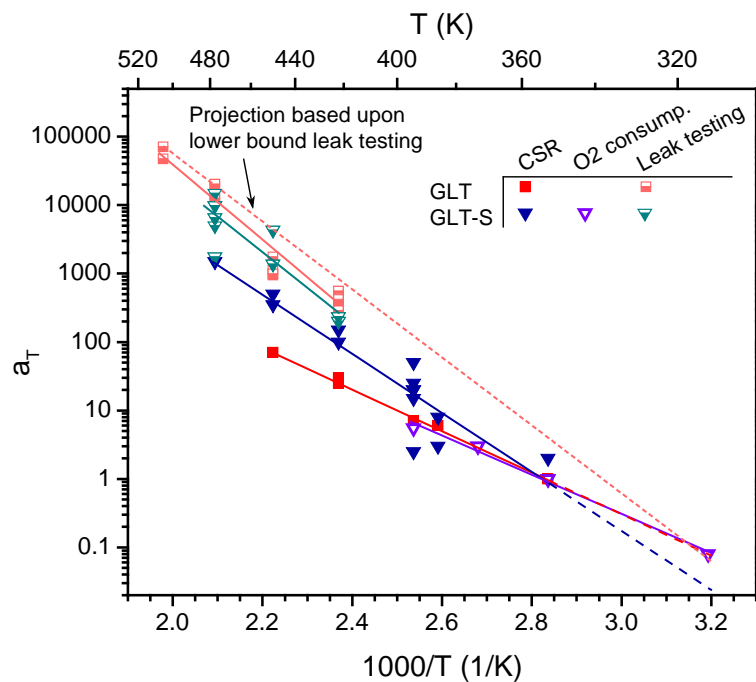


**Figure 12.** Plot of the shift factors ( $a_T$ ) for CSR, oxygen consumption (0.13 inch thickness), and leak testing of GLT and GLT-S samples. The dashed lines are projected shift factor values.

#### 4.0 Conclusions

CSR testing continues for GLT and GLT-S O-ring samples at 175 and 250 °F. Oxygen consumption testing continues for GLT-S O-ring samples at 73 to 250 °F. The bounding average

O-ring temperature expected in the KAC is 158 °F, based on an average ambient temperature of 95 °F and the maximum payload (19 W). Cooler ambient temperatures and reduced payloads are less damaging to the seals. The data available to date suggest the GLT and GLT-S O-rings have potential service life at 158 °F of up to 34 years and 570 years, respectively.

Data from oxygen consumption are generally in agreement with results from compression stress relaxation testing and leak testing. The oxygen consumption testing includes results from temperatures near KAC service temperatures and corroborates and adds confidence in predictive models based on mechanical testing. However, uncertainty still exists in extrapolating these elevated temperature results to the KAC service temperatures due to sample variation in testing results and the effect of diffusion-limited oxidation on the samples. Aging and CSR testing will continue for GLT and GLT-S O-ring samples at 175 and 250 °F. Aging and oxygen consumption testing will continue for GLT-S O-ring samples at 73 to 250 °F, and oxygen consumption testing might commence for GLT O-ring samples.

## 5.0 References

1. WSRC-SA-2002-00005, Rev. 10, "K Area Complex Documented Safety Analysis", June 2014.
2. M-CLC-K-00788, "The Initial and 20-year Service Thermal Performances of the 9975 Shipping Packages due to Fire-Drop-Smoldering Accidents in KAC", Kiflu, B.B., January 2017.
3. M-CLC-K-00789, "The Initial and 20-year Service Thermal Performances of the 9975 Shipping Packages due to Fire Accident in KAC Facility", Kiflu, B.B., January 2017.
4. M-CLC-K-00786, "Dynamic Analysis of 30-ft Drop for 9975 Package in Storage Conditions", Johnson, J., January 2017.
5. M-CLC-K-00787, "Structural Analysis of the 9975 Package for a Facility Condition Forklift Accident with 20 year Aged Package Conditions", McKeel, C., January 2017.
6. SRNL-TR-2014-00057, "Task Technical and Quality Assurance Plan for Characterization and Surveillance of Model 9975 Shipping Package O-Rings and Fiberboard Materials", April 2014.
7. WSRC-TR-2001-00286, Rev. 9, "The Savannah River Site Surveillance Program for the Storage of 9975/3013 Plutonium Packages in KAC", September 2017.
8. SRNL-STI-2015-00683, "CSR Behavior and Aging Model for the Viton® Fluorelastomer O-Rings in the 9975 Shipping Package", McWilliams, A.J., W.L. Daugherty, and T.E. Skidmore.
9. Gillen, K.T., M. Celina, and R. Bernstein, *Validation of improved methods for predicting long-term elastomeric seal lifetimes from compression stress-relaxation and oxygen consumption techniques*. Polymer Degradation and Stability, 2003. **82**(1): p. 25-35.
10. Assink, R.A., et al., *Use of a respirometer to measure oxidation rates of polymeric materials at ambient temperatures*. Polymer, 2005. **46**(25): p. 11648-11654.

11. Celina, M.C., *Review of polymer oxidation and its relationship with materials performance and lifetime prediction*. Polymer Degradation and Stability, 2013. **98**(12): p. 2419-2429.
12. WSRC-TR-2004-00331, "Baseline Compression Set and Stress-Relaxation Behavior of Model 9975 Shipping Package O-rings", Skidmore, T.E., December 2004.
13. Ronan, S., et al., *Long-term stress relaxation prediction for elastomers using the time-temperature superposition method*. Materials & Design, 2007. **28**(5): p. 1513-1523.
14. SRNL-TR-2017-00257, "FY2017 Status Report: Model 9975 O-Ring Fixture Long-Term Leak Performance", Daugherty, W.L., July 2017.
15. Gillen, K.T. and M. Celina, *The wear-out approach for predicting the remaining lifetime of materials*. Polymer Degradation and Stability, 2000. **71**(1): p. 15-30.

## Appendix A

**Table A-1.** Sample information for vessels used in oxygen consumption testing.

Aging temperature (°F)	# of Pieces	Thickness (in)	Total weight (g)	Vessel free volume (cc)
73	4	0.03	1.433	19.7
	2	0.07	1.682	19.4
	3	0.13	4.247	19.4
104	3	0.13	4.490	20.5
	5	0.07	4.231	19.6
140	5	0.07	4.165	19.7
	1*	0.21	0.694	19.8
175	3	0.13	4.284	18.1
	5	0.07	4.247	19.6
212	8	0.03	2.733	20.5
	8	0.03	2.899	18.8
	2	0.13	2.827	18.9
	4	0.07	3.338	18.7
250	1	0.13	1.364	19.8
	2	0.07	1.632	19.5
	4	0.03	1.440	20.8
	1*	0.21	0.698	19.8

\*EPDM sample

**Table A-2.** Shift factors for TTS plots of CSR and oxygen consumption results.

Aging temperature	CSR				Oxygen consumption			
	GLT		GLT-S		Aging temperature	a <sub>T</sub> (GLT-S)		
	Jig #	a <sub>T</sub>	Jig #	a <sub>T</sub>		0.03"	0.07"	0.13"
175 °F	J-8	1	J-52	1	104 °F		0.14	0.08
	J-1B	1	J-51	2	140 °F		0.36	
235 °F	J-2B	6	J-54	3	175 °F		1	1
	J-9	6	J-53	8	212 °F	1.8	1.9	3
250 °F	J-17	7	J-86H	2.5	250 °F	3.2	4.5	5.5
	J-3B	7	J-55	20				
	J-10	7	J-56	50				
	J-16	7	J-57	15				
	J-83H	7	J-58	25				
			J-59	20				
300 °F	J-18	30	J-60	150				
	J-4B	25	J-61	100				
350 °F	J-21	70	J-62	350				
	J-7B	70	J-63	500				
400 °F			J-25	1,500				
			J-6B	1,500				

**Table A-3.** Time to failure [14] and shift factors for leak testing results.

Aging temperature (°F)		Fixture ID	Days to failure		Shift factor, normalized to 300 °F		Shift factor, shifted so $a_T=1$ at 175 °F	
			Inner	Outer	Inner	Outer	Inner	Outer
GLT	300	8	2,082	2,082	0.6	0.6	271	271
		12	1,020	1,020	1.3	1.3	554	554
		26	1,366	1,273	0.9	1.0	414	444
		30	1,392		0.9		406	
		31	1,291	1,291	1.0	1.0	438	438
		32	1,352	1,352	1.0	1.0	418	418
		33	1,466	1,979	0.9	0.7	385	286
		49	1,276	1,360	1.0	0.9	443	415
	350	18D	497	324	2.6	4.0	1,137	1,744
		19D	594	571	2.2	2.3	951	990
	400	14D	45	45	28.7	28.7	12,556	12,556
		21D	28	28	46.1	46.1	20,180	20,180
	450	23D	12	8	107.6	161.4	47,087	70,630
GLT-S	300	29H	2,455	2,455	0.9	0.9	201	201
		34H	2,096	2,096	1.1	1.1	236	236
	350	38H	358	358	6.2	6.2	1,380	1,380
		39H	114	114	19.6	19.6	4,332	4,332
	400	45H	99	33	22.6	67.7	4,989	14,966
		58H	75	75	29.8	29.8	6,585	6,585
		60H	50	50	44.7	44.7	9,877	9,877
		62H	50	50	44.7	44.7	9,877	9,877
		28H	50	50	44.7	44.7	9,877	9,877
		50H	281	281	7.9	7.9	1,758	1,758

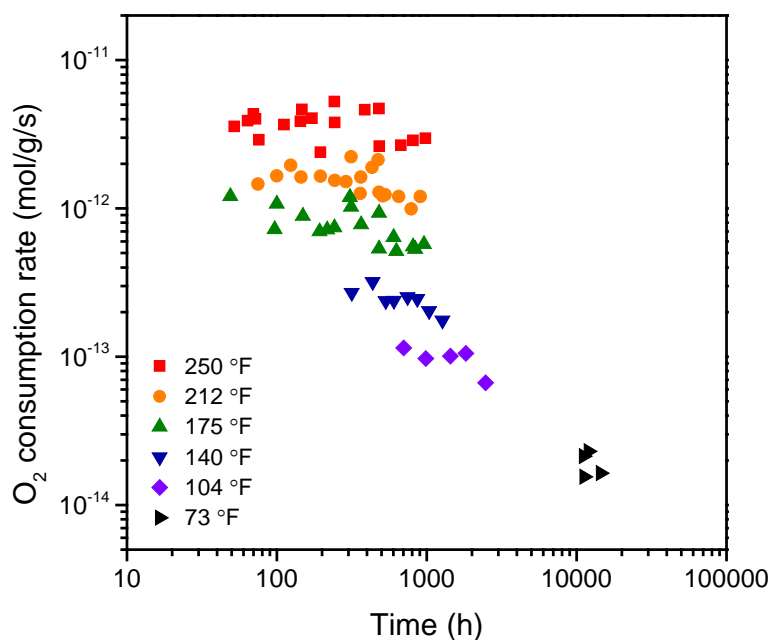


**Figure A-1.** Oxygen consumption rate results for 0.07 inch thick GLT-S samples.

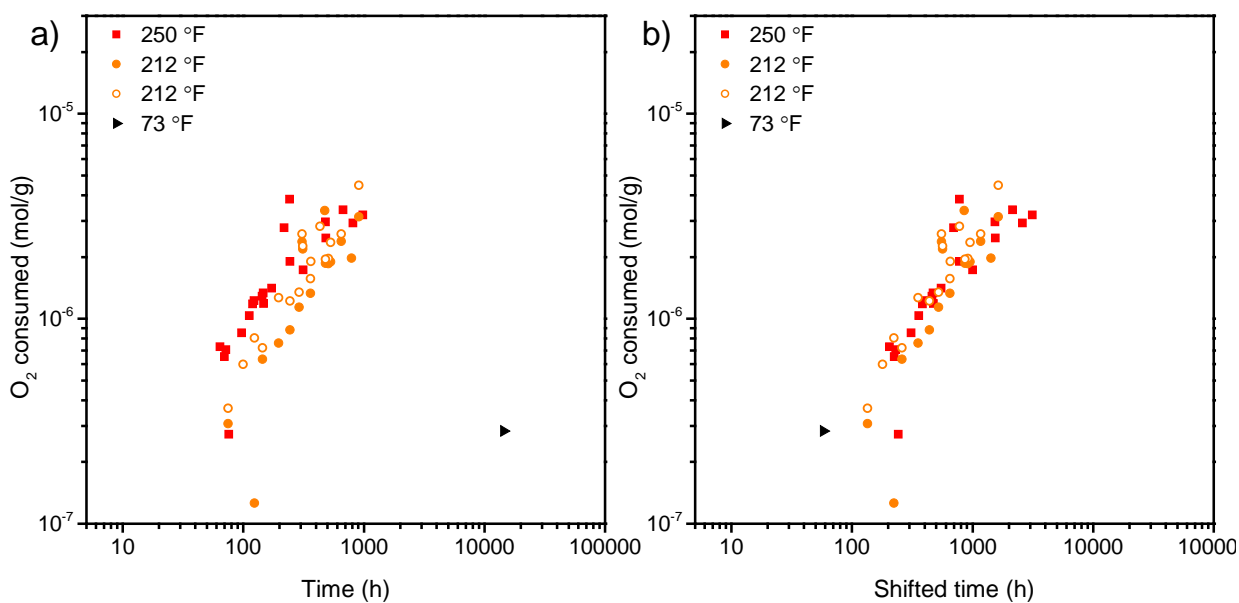


**Figure A-2.** The oxygen consumption (a) and time-temperature superposition of oxygen consumption data relative to 175 °F,  $a_T=1$  (b) for 0.03 inch thick GLT-S samples.



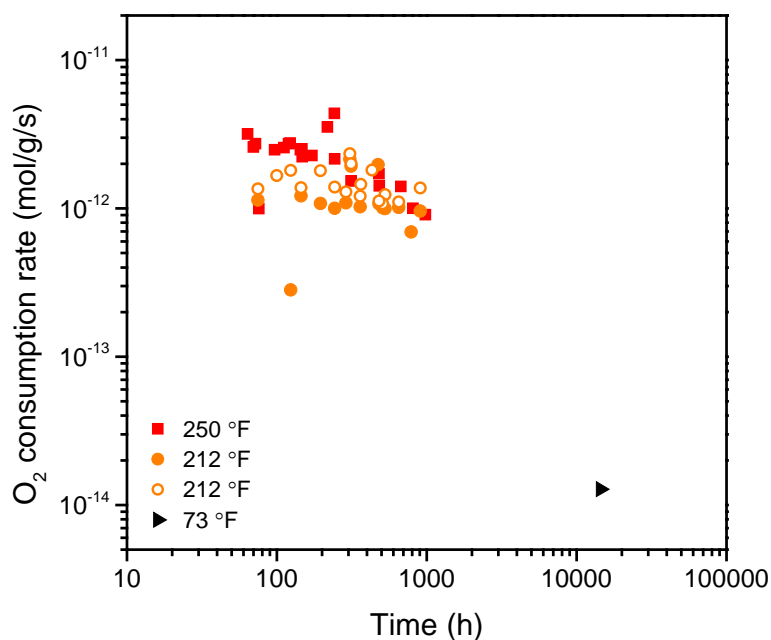


**Figure A-3.** Oxygen consumption rate results for 0.03 inch thick GLT-S samples.

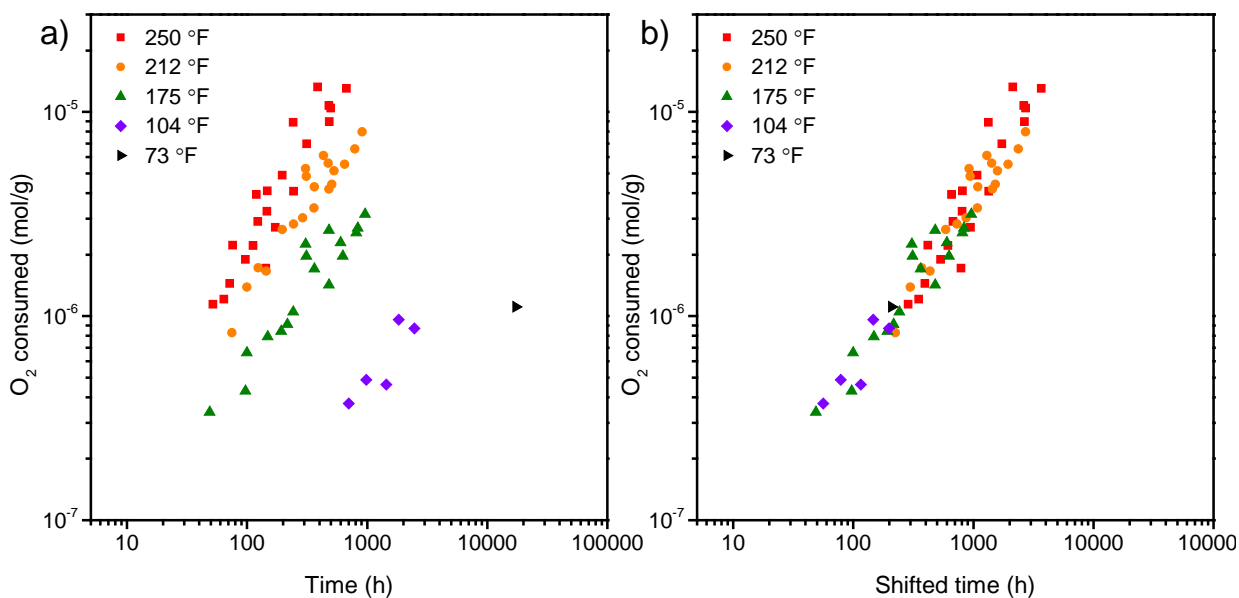


**Figure A-4.** The oxygen consumption (a) and time-temperature superposition of oxygen consumption data relative to 175 °F,  $a_T=1$  (b) for 0.13 inch thick GLT-S samples.

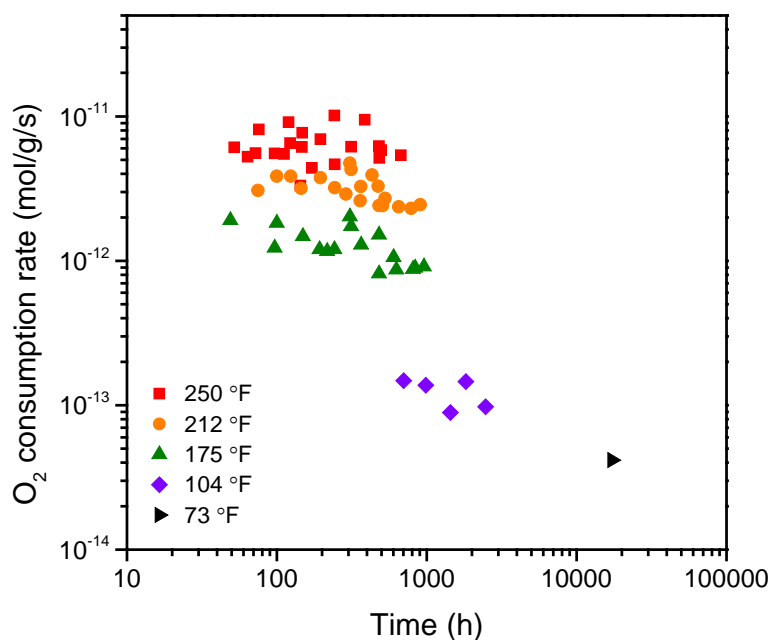


**Figure A-5.** Oxygen consumption rate results for 0.13 inch thick GLT-S samples.

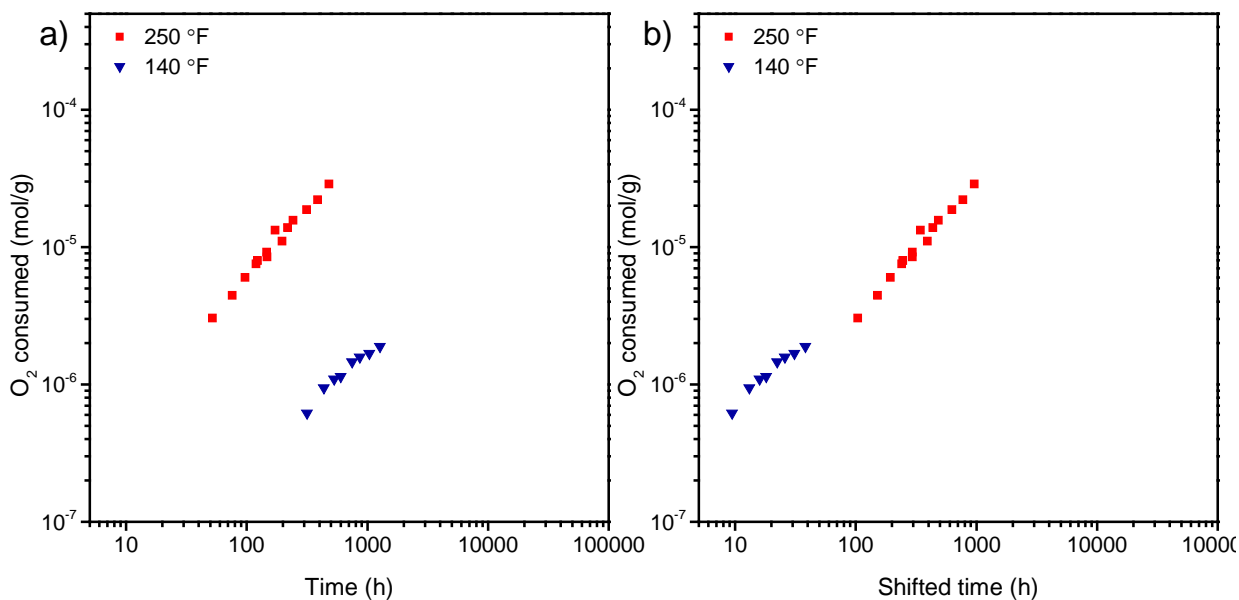


**Figure A-6.** The oxygen consumption (a) and time-temperature superposition of oxygen consumption data relative to 175 °F,  $a_T=1$  (b) for EPDM samples.

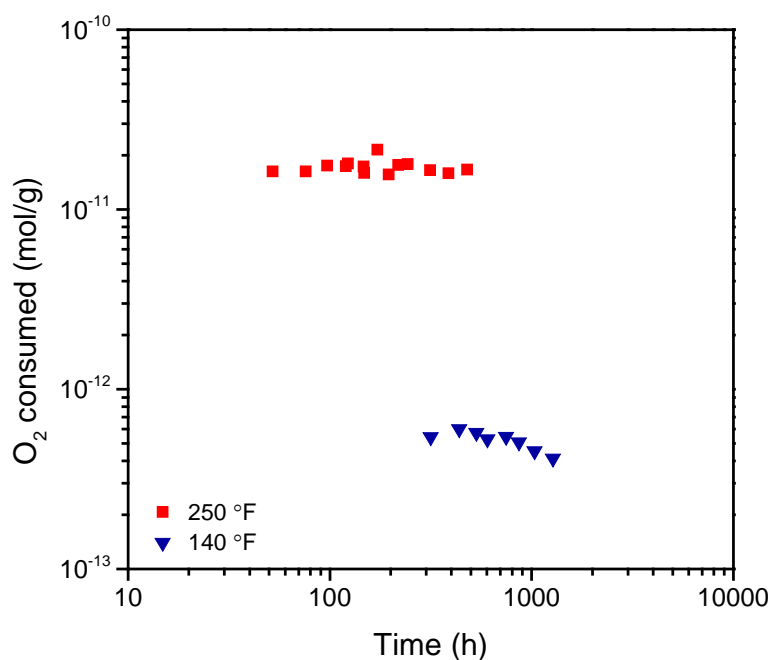


**Figure A-7.** Oxygen consumption rate results for EPDM samples.

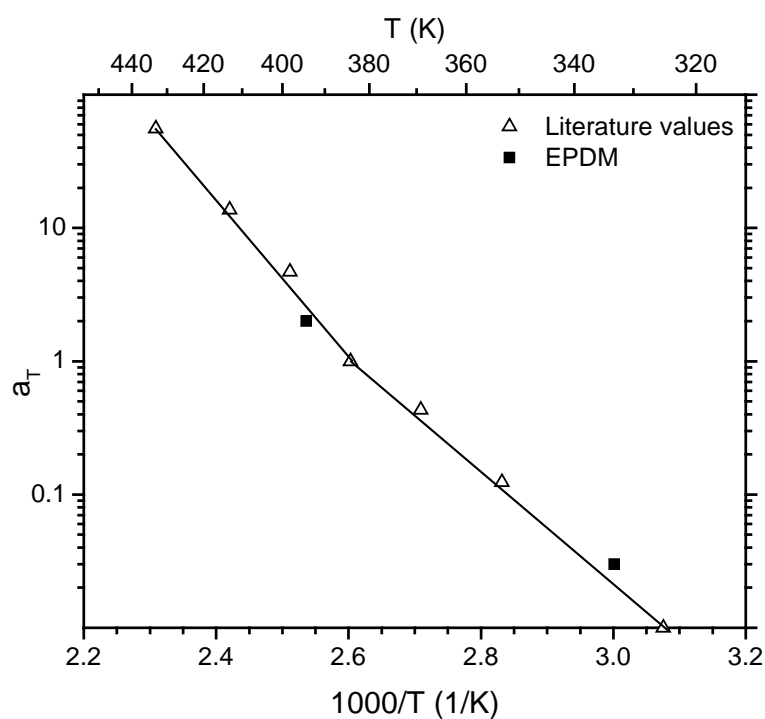


**Figure A-8.** Comparison of the shift factors ( $a_T$ ) for oxygen consumption data of EPDM to reported values [15].

**Distribution:**

G.A. Abramczyk, 730-A  
R. J. Bayer, 705-K  
J.S. Bellamy, 730-A  
W.L. Daugherty, 773-A  
B.A. Eberhard, 105-K  
B. L. Garcia-Diaz, 999-2W  
T.W. Griffin, 705-K  
R. J. Grimm, 705-K  
E.R. Hackney, 705-K  
S.J. Hensel, 705-K  
J. M. Jordan, 705-K  
B. B. Kiflu, 705-K  
M. D. Kranjc, 730-A  
D.R. Leduc, 730-A  
P. L. Livengood, 705-K  
J.W. McEvoy, 707-C  
A.J. McWilliams, 773-A  
P. M. Palmer, 705-K  
M. M. Reigel, 773-A  
T.E. Skidmore, 730-A  
T. T. Truong, 773-41A  
K.E. Zeigler, 773-41A  
Document Control